Multivalent metal tetrahydroborides of Al, Sc, Y, Ti, and Zr

Zbigniew Łodziana*

EMPA Swiss Federal Institute for Materials Testing and Research, Hydrogen and Energy, Überlandstrasse 129, Dübendorf, Switzerland and Institute of Nuclear Physics, Polish Academy of Sciences, ul. Radzikowskiego 152, PL-31-342 Kraków, Poland

(Received 8 January 2010; revised manuscript received 2 March 2010; published 13 April 2010)

Metal tetrahydroborates remain interesting materials as potential hydrogen storage media. While overcoming large thermodynamic stability of uni- and divalent metal borohydrides may still be challenging, very little information is available about tetrahydroborates of tri- or tetravalent metal cations. Here, we analyze basic thermodynamic and electronic properties of borohydrides of Al, Sc, Y, Ti, and Zr by means of extensive density functional calculations. We show that solid phases of these compounds can range from ionic-like structures for $Y(BH_4)_3$ to the molecular ones of $Al(BH_4)_3$ and $Zr(BH_4)_4$. These compounds are thermodynamically unstable at room temperature with respect to their decomposition into boron and hydrogen. Their stability is explained through the experimentally observed formation of diborane being a necessary step in the decomposition path. This points out that the kinetic factors are important for analysis of the metal borohydrides stability.

DOI: 10.1103/PhysRevB.81.144108 PACS number(s): 65.40.−b, 68.60.Dv, 71.15.Nc

I. INTRODUCTION

Two groups of complex metal hydrides: tetrahydroaluminates containing AlH_4 groups and tetrahydroborates with BH_4 groups have been recently under intensive study, due to their potential hydrogen storage capabilities. As boron is ~2.5 times lighter than aluminum tetrahydroborates (also referred as borohydrides or boranates) seem more appealing for practical application for efficient hydrogen storage.[1,2] Unfortunately, there is no known metal borohydride that possesses both thermodynamic and kinetic properties suitable for such purposes (i.e., reversible hydrogen release below $T \sim 400$ K at 1 bar hydrogen pressure).

Borohydrides of alkali and alkaline earth metals form ionic solids consisting of metal cation and a negatively charged BH_4^- group. The stoichiometry of these compounds reflects the valency of metal cations, i.e., MBH_4 and $M(BH_4)_2$ for alkali and alkaline earth metals, respectively. Both groups of borohydrides are stable; at ambient conditions they remain in a solid crystalline form,[3–8] and they decompose in temperature above 500 K. Tetrahydroborates of alkaline earth metals are structurally more complex than those of alkali metals.

Among borohydrides containing metal cation with the valency larger than two, $Al(BH_4)_3$ is a volatile liquid at ambient conditions (it decomposes spontaneously).[9–15] $Y(BH_4)_3$ has been recently synthesized in the crystalline solvent free phase[16] and has been shown to be stable well above room temperature. The crystalline solid form of $Ti(BH_4)_3$ decomposes spontaneously at ambient conditions,[17] and $Zr(BH_4)_4$ crystallizes in $P\bar{4}3m$ symmetry and is stable below 302 °C.[18]

In general, the stability of borohydrides containing metals at third or fourth oxidation state is lower than in the case of respective compounds of metals with lower valency. Unfortunately, structural and thermodynamic properties of these compounds are relatively less known, even though they were intensively studied in the past in the gaseous form or in liquid solutions.[17]

In the present paper, we study thermodynamic and electronic properties of selected trivalent and tetravalent metal tetrahydroborates by means of density-functional theory (DFT) calculations. We focus our attention on five cations: Al, Sc, Y, Ti, and Zr. We show that tetrahydroborates of Al, Sc, Ti, and Zr are thermodynamically unstable with respect to decomposition into hydrogen and boron. Their stability at ambient conditions can be explained through the formation of diborane (B_2H_6) as a necessary step in the decomposition path. Diborane possesses positive formation enthalpy, but is kinetically robust at ambient conditions. In the gas phase B_2H_6 decomposes spontaneously into higher boranes and hydrogen above 323 K and disintegrates into elements above 673 K.[19] Higher boranes are observed as decomposition products of borohydrides of alkali and alkaline earth metals that decompose at temperatures well above 500 K.[20–25] This is especially significant for $[B_{12}H_{12}]^{2-}$ that forms salts with exceptional stability.[23–25] While the appearance of these stable compounds is determined by their thermodynamic stability, formation of diborane points at the kinetic effects that are important for considerations about stability of borohydrides. Taking into account molecular and crystalline forms of these compounds we show that $Al(BH_4)_3$ and $Zr(BH_4)_4$ form a crystalline structure via weak Van der Waals interaction of the stoichiometric units, while other compounds possess a crystalline form not related to their stoichiometric molecular structure. The structural properties of the studied compounds are related to the properties of metal cations that govern the local coordination number for metals. The orientation of BH_4 groups in $Al(BH_4)_3$ is explained by a simple electrostatic model.

II. METHOD

The present calculations were performed with the periodic plane wave DFT approach.[26,27] The plane wave method is used since it allows for a straightforward comparison between periodic solids and isolated molecules. The valence configurations $1s^1$ for H; $2s^22p^1$ for B; $3s^23p^1$ for Al; $3p^64s^23d^1$ for Sc; $4s^24p^65s^24d^1$ for Y; $3p^63d^24s^2$ for Ti and $4s^24p^65s^24d^2$ for Zr were represented by projected augmented wave potentials.[28,29] The spin polarized generalized

gradient approximation (GGA) was used for the exchange-correlation functional.[30] Energy cutoff of 1000 eV and in the case of solids k-point grid with spacing of 0.05 $Å^{-1}$ were applied. For isolated molecules and gaseous hydrogen the calculations were performed in the cubic box with the edge of 20 Å. The ground-state electronic density was determined by iterative diagonalization of the Kohn-Sham Hamiltonian and Gaussian smearing of 0.1 eV was applied. Atomic positions and unit cell parameters for the solids were relaxed with conjugated gradient algorithm until the forces exerted on atoms were smaller than 0.005 eV/Å. Normal mode analysis was performed for all molecular systems and for solids at the Γ point by finite atomic displacements of the order of ± 0.02 Å.

The finite temperature properties were calculated within harmonic approximation.[31] The vibrational Helmholtz free energy is calculated as

$$F_v(T) = k_B T \sum_i g(\omega_i) \ln\left[2 \sinh\left(\frac{\hbar\omega_i}{2k_B T}\right)\right]. \quad (1)$$

The sums run over $3N-3$ degrees of freedom for the solid phases, N is the number of independent atoms in the primitive unit cell or in the molecular unit. For linear molecular units two rotational degrees of freedom are silent and the sum runs over $3N-5$ degrees of freedom. ω_i is the frequency of mode i, $g(\omega_i)$ stands for density of states, k_B is Boltzmann constant and T—temperature.

Thermodynamic stability of phases is compared via Gibbs free energy,

$$G(T,p) = F(T) + pV, \quad (2)$$

where the free energy reads,

$$F(T) = E_0 + F_v(T). \quad (3)$$

E_0 is the electronic ground-state energy for relevant species. For the solid phases and the pressure range considered here the pressure-volume dependence is negligible and pV term relates to gaseous species only.

For diatomic hydrogen the free energy can be expressed as[32,33]

$$\mu_{H_2} = E_0^{H_2} + kT\left(\ln\frac{pV_Q}{kT} - \ln Z_{rot} - \ln Z_{vib}\right), \quad (4)$$

where $V_Q = \sqrt{(h^2/2\pi mkT)^3}$ is the quantum volume. Numerical value for μ_{H_2} reads as

$$\mu_{H_2} = 8.314512 \cdot 10^{-3} T \ln\{1.267865 \cdot 10^3 pT^{-7/2} \times [1 - \exp(6.301215 \cdot 10^3)/T]\} + 25.972191 \ \text{(kJ/mol)},$$

the $E_0^{H_2}$ is the electronic ground-state energy for a hydrogen molecule. Thus, for hydrogen $G(T,p) = N\mu_{H_2}$, where N is the number of H_2 molecules in the considered system.

The valence charge analysis was performed with the Bader method[34,35] and for each system a separate set of calculations was performed with an accurate electronic charge density represented on the grid of at least $\Delta x \simeq 0.025$ Å. The dipole moments for the molecular units were calculated using the electron density distribution in the real space.

III. RESULTS

A. Solid state structures

Complex borohydrides of univalent and divalent cations form ionic solids, and a large variety of their physicochemical properties are known for the low-temperature crystalline phases. For example, the low-temperature phase of $LiBH_4$ has *Pnma* symmetry and Li cations are coordinated by four BH_4 groups.[3,36–38] Sodium and potassium borohydrides ($NaBH_4$, KBH_4) have $P4_2/nmc$ symmetry and their metal cations adopt octahedral coordination.[5,39,40] For divalent cations the structures of $Be(BH_4)_2$,[41] $Mg(BH_4)_2$,[6,7,42–46] and $Ca(BH_4)_2$ (Refs. 8 and 47–52) have been recently reported. In calcium borohydride Ca cations are octahedrally coordinated to the surrounding BH_4 groups for all reported crystalline phases of this compound.[8,47–51] The structure of magnesium borohydride is still disputed. The experimentally proposed low-temperature α phase consists of 330 atoms in the unit cell with $P6_1$ symmetry[6,7] (this structure has been recently revised to $P6_122$ structure[44]). On the other hand, theoretically predicted phases consist of significantly smaller and simpler unit cells.[42,43,45,46] In his recent paper, however Voss *et al.*[43] points out that fine details of the structure are unimportant for description of thermodynamic properties of this compound.

For univalent and divalent cations their known borohydrides have tetrahedral (for Li and Mg) and octahedral (for Na, K, and Ca) coordination.[53] At higher temperatures these compounds undergo phase transitions, often becoming disordered.[4,54,55] All these compounds are relatively stable and they decompose into metal hydrides and hydrogen only at temperatures above 500 K. Formation of diborane was also reported for $LiBH_4$.[20]

The structural and thermodynamic properties of metal borohydrides with tri- or tetravalent cations are relatively less known, even though these compounds were intensively studied in their gas/molecular phases.[17] Below, we focus our attention on selected borohydrides of tri-(Al, Sc, Y, Ti) and tetravalent (Ti, Zr) metal cations in their crystalline and molecular forms. Such a distinction is done to assess the accuracy of calculations, which are performed for the single gas phase molecular structures and compared to solid state phase.

At ambient conditions the lightest trivalent borohydride $Al(BH_4)_3$ is a liquid;[10–13] borohydrides of scandium,[17,56] titanium,[17,57–59] and zirconium[18,22,60–63] were reported as volatile solids at RT that decompose spontaneously in the case of $Ti(BH_4)_3$. In the past the molecular properties of these compounds were intensively studied in a liquid solution or by computational chemistry methods.[12,17,59] In our present studies for the compounds with known structure we use the symmetry of the low-temperature phase. As the purpose of the present studies is not to find or propose unknown ground state symmetries, we consider the model crystalline state for $Sc(BH_4)_3$, $Ti(BH_4)_3$ for comparison purposes only. Properties of solid phases are compared with a molecular form of each compound.

Two structural polymorphs of the low-temperature solid phase of $Al(BH_4)_3$ are known: α phase with $C2/c$ (no. 15)

symmetry and β phase with $Pna2_1$ (no. 33) symmetry.[13,64] Both crystalline forms have aluminum atoms coordinated to three BH_4 groups. Thus the basic structural building block has the stoichiometry of this substance. Indeed, the formation enthalpy of the crystalline structure is only 9.6 kJ/mol larger than that of the isolated $Al(BH_4)_3$ molecular unit. Such a feeble binding of the crystal is a clear indication of weak dispersive Van der Waals forces responsible for the formation of the solid. The heat of vaporization for $Al(BH_4)_3$ was estimated as ~30 kJ/mol,[14,15] and that compares well with the present calculations. Below, we focus our attention on β phase of $Al(BH_4)_3$ and the optimized structural parameters are presented in the supporting material.

Scandium borohydride, synthesized via wet chemical methods, was reported as a volatile white solid, sublimable at 80 °C.[17,56] No experimental details of the structure were reported for this compound, and the recent theoretically predicted structure of $Sc(BH_4)_3$ possesses $C222_1$ (no. 20) symmetry.[65] For the purpose of the present studies we have calculated electronic and thermodynamic properties of $Sc(BH_4)_3$ in the cubic structure of yttrium borohydride, which we found to be more stable (by 32 kJ/mol per formula unit) than $R\bar{3}$ structure proposed by Nakamori *et al.*[66] The orthorhombic structure[65] has been also considered in the present studies. It is more stable than the cubic one (by ~14 kJ/mol); however, the density of the cubic phase is much larger, 1.057 g/cm^3 compared to 0.722 g/cm^3 for the orthorhombic one. The differences between those hypothetical phases of $Sc(BH_4)_3$ are discussed at the end of this paper. The ground state orthorhombic crystalline phase is by 60 kJ/mol more stable than the isolated stoichiometric $Sc(BH_4)_3$ molecular unit.

$Y(BH_4)_3$ has been recently synthesized via metathesis reaction in a solvent free-crystalline phase with $Pa\bar{3}$ cubic symmetry.[16] In this structure, metal cations are coordinated to six nearest neighbors. Thus this structure cannot be considered as a crystal consisting of molecular $Y(BH_4)_3$ units. The decomposition of yttrium borohydride starts around 450 K.[16] The ground-state crystalline phase is more stable by 128 kJ/mol then isolated stoichiometric molecular unit. The structural details of $Y(BH_4)_3$ and $Sc(BH_4)_3$ are presented in the supporting material.

The cubic $P\bar{4}3m$ (no. 215) structure of $Zr(BH_4)_4$ was proposed experimentally[60] and reported recently on the basis of quantum calculations.[66] In this structure, Zr cation is coordinated to four BH_4 groups, that are equivalent to a stoichiometric unit of this compound. The ground-state energy of the crystalline phase is ~10 kJ/mol lower than the respective energy for the isolated molecular $Zr(BH_4)_4$ units. This indicates that dispersive forces are responsible for the crystallization, similarly as in the aluminum borohydride. We have found that the crystalline form of $Zr(BH_4)_4$ with $R3$ symmetry is 10 kJ/mol more stable than the cubic $P\bar{4}3m$ phase. The structural details for both phases are provided in the supporting material.

Titanium borohydride was reported as a highly air sensitive green solid that decomposes autocatalytically at 25 °C.[17,57] Stoichiometry of this compound is $Ti(BH_4)_3$ and the details of molecular structure were reported in Refs. 18 and 59. However, we are not aware of any reports concerning the structure of the crystalline phases of $Ti(BH_4)_3$ or $Ti(BH_4)_4$. For comparison purposes a hypothetical solid phase $Ti(BH_4)_3$ in the $C222_1$ symmetry is considered in the present paper.

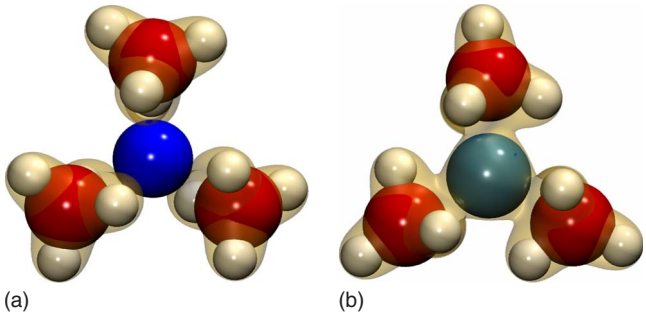

FIG. 1. (Color online) Molecular structure of $Al(BH_4)_3$ (a) and $Ti(BH_4)_3$ (b). Light gray (blue) spheres are for metal cation, dark gray (red) ones—boron, and small white balls represent hydrogen. The haze around atoms shows the electron density isosurface at 0.35 e/Å^3.

A relatively weak binding of some crystalline phases indicates that their thermodynamic properties are dictated by the properties of the constituent molecular units of metal borohydrides and not by the cohesive crystal energy. In the following paragraphs, we focus our attention on structural, electronic and thermodynamic properties of isolated $M(BH_4)_x$ with $x=2,3,4$ molecular units and on selected crystalline forms of these compounds. Such an approach provides a good comparison between molecular and crystalline forms and gives a lower boundary for the stability of compounds.

To study thermodynamic stability of metal borohydrides we have calculated the ground state and vibrational energy of all relevant binary metal hydrides, as well as for B_2H_6 and B_4H_{10}. For reference, we have considered the following compounds, AlH_3 with $R\bar{3}c$ (no. 167) symmetry and optimized lattice parameters $a=4.44$ Å, and $c=11.93$ Å. The other hydrides were considered in the cubic symmetry $Fm\bar{3}m$ (no. 225) of fluorite structure and the optimized lattice parameters are: $a=4.78$ Å for ScH_2; $a=5.22$ Å for YH_2; $a=4.43$ Å for TiH_2, and $a=4.82$ Å for ZrH_2.

B. Molecular structure

In this section, the structural properties of molecular gas phase metal borohydrides are presented. The molecular aluminum tetraborohydride ($Al(BH_4)_3$) possesses a planar structure with D_3 symmetry.[11,12] The BH_4 units are arranged in bidentate orientation—two hydrogen atoms are pointed toward Al and they are rotated ~17° around Al–B axis, see Fig. 1(a). Without such a rotation the higher D_{3h} symmetry of this molecule shall be observed.[12] The structure of both Ti- and Zr-based borohydride molecules is also well characterized. In these compounds the tridentate arrangement of BH_4 (three hydrogen atoms pointing toward metal) is preferred. $Ti(BH_4)_3$ forms a planar molecule with C_{3h} symmetry and BH_4 groups that are rotated by a small angle with respect

TABLE I. Structural parameters for metal BH_4 [$M(BH_4)_x$; M=Al,Sc,Y,Ti,Zr] complexes, d is a distance between metal and boron atom. The γ stands for boron-metal-boron $\angle_{B-M-B}$ angle. The dipole moment is given in Debyes.

	$(BH_4)_2$			$(BH_4)_3$			$(BH_4)_4$		
Ion	d (Å)	γ (deg)	μ_D (D)	d (Å)	γ (deg)	μ_D (D)	d (Å)	γ (deg)	μ_D (D)
Al	2.10	132.73	0.42	2.14 (2.14[a])	120	0.09			
Sc	2.23	179.61	0.02	2.26	120	0.02			
Y	2.40	180	0.01	2.43	120	0.05			
Ti	2.14	180	0.01	2.15 (2.17[b])	120	0.00	2.17	109.47	0.00
Zr	2.29	180	0.01	2.30 (2.31[b])	120	0.00	2.32	109.47	0.00

[a]Reference 11.
[b]Reference 57.

to fully symmetric orientation,[57,59] see Fig. 1(b). $Zr(BH_4)_4$ possesses the T_d symmetry[62] that is preserved also in the crystalline structure.[60] According to our knowledge structural properties of $Sc(BH_4)_3$ and $Y(BH_4)_3$ molecules have not been reported before.

We have calculated equilibrium properties for compounds with all the metals investigated in the present study and with the stoichiometry ranging from $M(BH_4)_2$ to $M(BH_4)_4$, (M=Al,Sc,Ti,Y,Zr). This range of stoichiometries allows us to determine the stability with respect to desorption/adsorption of BH_4. The structural parameters for the optimized geometries for each stoichiometry are presented in Table I.

For the $M(BH_4)_2$ stoichiometry the transition metals and yttrium cations form linear molecules. These molecules do not have any dipole moment, see Table I. For aluminum the molecule is bent due to a short Al–B distance; $Al(BH_4)_2$ possesses a dipole moment of 0.42 D. A small deformation is also present for $Sc(BH_4)_2$.

The structures containing three BH_4 groups form planar molecules with boron atoms arranged on an equilateral triangle around the central metal. BH_4 groups have bidentate orientation for Al and tridentate orientation for all other elements considered here. The dipole moment for this composition is very small and does not exceed μ_D=0.09 D (compared to 1.85 D for H_2O) for $Al(BH_4)_3$, see Table I.

In the fourth oxidation state, only molecules of borohydrides with Ti and Zr cations are stable at T=0 K. They form a tetrahedral structure with boron atoms at the vertices and the metal atom in the center. The BH_4 are arranged in tridentate orientation. Both compounds have the stoichiometry compatible with a preferred oxidation state of the metal and they possess no dipole moment, see Table I.

The metal boron bond length increases slightly with the increasing number of BH_4 groups for all metals. It is interesting to notice that for aluminum and titanium the Al–B and Ti–B distances are very similar (Table I). However, structural thermodynamic and electronic properties of these compounds differ significantly.

The range of compositions for molecular borohydrides considered here allows us to gain insight into their most stable stoichiometry. This is done by comparing the ground state energy (including zero point vibrations) in the following reactions: $M(BH_4)_n \Leftrightarrow M(BH_4)_{n-1}+B+2H_2$, with n=3 for all metals and, additionally, n=4 for Ti and Zr. As expected, $Al(BH_4)_3$ is stable with respect to detachment of BH_4 by 183 kJ/mol, $Sc(BH_4)_3$ by 178 kJ/mol; $Y(BH_4)_3$ by 201 kJ/mol. For transition metals detachment of the BH_4 from $M(BH_4)_3$ is also endothermic by 198 kJ/mol for Zr and 137 kJ/mol for Ti. However, for the last two elements the association of additional BH_4 is exothermic by 125 kJ/mol for Zr, and only by 25 kJ/mol for Ti. A relatively low stability of $Ti(BH_4)_4$ with respect to $Ti(BH_4)_3$ suggests that at finite temperatures entropic factors may serve as a driving force toward stoichiometry change. Indeed, within the harmonic approach $Ti(BH_4)_3$ becomes thermodynamically stable with respect to $Ti(BH_4)_4$ above $T \sim 140$ K. This aspect will be discussed below.

1. Charge distribution

Analysis of the electronic charge density distribution gives an opportunity to get insight into the nature of bonding between atoms. The charge distribution calculated according to the Bader method[34,35] for all compounds and stoichiometries considered in the present studies is presented in Table II. A relatively large charge transfer between the metal cation and borohydride groups is observed for all compounds, and the ionic contribution to bonding is the largest for Al and Y coordinated to three BH_4 groups. For transition metals the charge transfer is smaller due to metal and BH_4 orbital hybridization.

For the compounds in the molecular form the positive charge on the metal atom increases accordingly to the increasing number of BH_4 groups. On the other hand, the charge distribution within each borohydride group depends only slightly on the stoichiometry for a given chemical composition. Especially the charge on a boron atom ranges only between +1.47 e for $Ti(BH_4)_2$ and +1.54 e $Al(BH_4)_3$. The distribution of electrons between hydrogen atoms shows a significant variation between H in the terminal position and those in the bridge positions between metal and boron. This difference is the largest for the compound containing Al with bidentate orientation for BH_4 and with charges on hydrogen at the bridge positions larger by ~0.14 e than the terminal ones. For other elements and tridentate BH_4 orientation these

TABLE II. Bader charges for Al, Sc, Y, Ti, Zr, and BH_4 complexes in units of electron charge. The symmetry of solid phases is given in the parentheses.

	$(BH_4)_2$			$(BH_4)_3$			$(BH_4)_4$		
Ion	Metal	Boron	Hygrogen	Metal	Boron	Hydrogen	Metal	Boron	Hydrogen
Al	+1.57	+1.48	−0.47/−0.63	+2.29	+1.54	−0.50/−0.64			
Al($Pna2_1$)				+2.30	+1.55	−0.51/−0.64			
Sc	+1.52	+1.55	−0.53/−0.60	+1.85	+1.54	−0.51/−0.55			
Sc($Pa\bar{3}$)				+1.90	+1.58	−0.55/−0.57			
Sc($C222_1$)				+1.83	+1.54/1.56	−0.53/−0.55			
Y	+1.56	+1.55	−0.60/−0.62	+2.03	+1.53	−0.51/−0.57			
Y($Pa\bar{3}$)				+2.06	+1.57	−0.56/−0.58			
Ti	+1.37	+1.47	−0.53/−0.55	+1.63	+1.51	−0.51	+1.85	+1.50	−0.48/−0.50
Ti($C222_1$)				+1.76	+1.56	−0.53/−0.55			
Zr	+1.42	+1.49	−0.52/−0.56	+1.82	+1.50	−0.50/−0.54	+2.17	+1.52	−0.49/−0.53
Zr($R3$)							+2.17	+1.55	−0.51/−0.53

differences do not exceed 0.05 e. Transition metals carry the charge lower by ~0.1, ~0.2 e than Al, Sc, or Y.

The charge distribution for $Al(BH_4)_3$ and $Zr(BH_4)_4$ between molecular and solid phases does not change. Stoichiometric molecular units are bound by ionic forces for Al and iono-covalent forces for Zr; these bonds are not perturbed by weak Van der Waals forces in the solid state. The molecular nature of $Al(BH_4)_3$ and $Zr(BH_4)_4$ results in a substantial vapor pressure for these compounds.[67] For compounds of Sc, Y, and Ti there is a noticeable change in the charge distribution between molecular and solid forms. In general, the charge transfer between metal and BH_4 increases for the solids (i.e., they become more ionic). Also, for compounds containing yttrium and scandium the charge distribution between hydrogen atoms becomes more homogeneous, see Table II.

2. *Tridentate orientation of* BH_4 *group*

In this section, we provide a simple explanation of how the bidentate BH_4 orientation in $Al(BH_4)_3$ results from the electrostatic repulsion between negatively charged hydrogen ions. Among all chemical compounds considered here, only $Al(BH_4)_3$ molecule possesses the bidentate orientation of BH_4 groups. The structural details of this molecular unit were discussed in the literature,[10–12] and there is an agreement that $Al(BH_4)_3$ forms a planar molecule with D_3 symmetry and all BH_4 groups are rotated by ~17° along Al–B axis with respect to the fully symmetrical D_{3h} structure.[12]

The Bader charge analysis presented above indicates that hydrogen atoms carry a negative charge that is larger than 0.5 e. This charge is the largest for $Al(BH_4)_3$, while for transition metals localization of the electronic charge density confined around H is smaller, and there is an overlap of electronic density between the metal and surrounding BH_4 units, see Fig. 1. The charge localization on BH_4 groups results in the electrostatic repulsion between them.

For the purpose of analyzing the electrostatic effects we assume that the charge on each hydrogen is the same. We consider each BH_4 group as a rigid body, i.e., we neglect a modification of BH_4 tetrahedral shape or B-H bond lengths. Each molecular group may rotate around the central boron atom and we describe this rotation by means of two angles, α is the rotation around axis perpendicular to the $Al(BH_4)_3$ molecule, while the second rotation axis is parallel to the metal-boron bond and is described by an angle β, as presented in Fig. 2(a). The BH_4 molecules are separated from the cation by a distance l that we express by the ratio of metal-B to B-H bond length. This ratio is ~1.7 for $Al(BH_4)_3$. The repulsive part of the electrostatic potential energy of the system can be expressed as $V=\Sigma_{i,j}\frac{q_H^2}{r_{i,j}}$, where $r_{i,j}$ runs over all hydrogen atoms of different BH_4 units (the interaction between H of the same BH_4 unit can be neglected, as the molecule is considered as a rigid body and this interaction will introduce an additive constant only). Furthermore we assume that the $Al(BH_4)_3$ molecule is symmetric, i.e., the orientation of each BH_4 molecular group is the same with respect to aluminum and can be expressed as $\mathbf{r}=\mathbf{R}_{\parallel}\cdot\mathbf{R}_{\perp}\mathbf{r}_0$, see also Ref. 53.

The potential energy of three BH_4 molecules surrounding Al is presented in Fig. 2(b). Within our choice of the initial conditions ($\alpha=\beta=0°$), the orientation of BH_4 is tridentate for angles $\alpha=0°$ and 250°13′. For $\alpha=125°06'$ and 305°06′, BH_4 groups are in bidentate orientation and for $\alpha=70°13'$ and 180° they are in monodentate orientation. One can see that pronounced energy minima are present for bidentate orientation at $\alpha=125°06'$ and a broad minimum for $\alpha=305°06'$. This simple model shows that the mutual repulsion of negatively charged hydrogen ions favors bidentate orientation for smaller molecules. This orientation is overruled by the orbital overlap in $Ti(BH_4)_3$, but is present in $Al(BH_4)_3$, even when modified by a small nonionic contribution. The broad minima in bidentate configuration have two local configurations with slightly tilted BH_4 and are practically flat for a small rotation around β axis. This is in accordance with the rotation of BH_4 by ~17° around Al–B axis,[12] caused by nonionic effects.

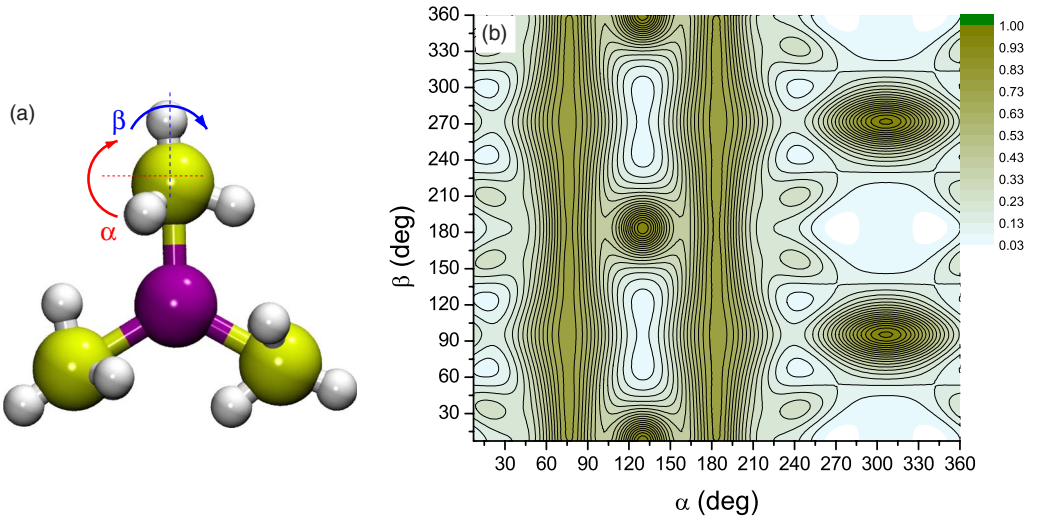

FIG. 2. (Color online) (a) Schematic view of the $Al(BH_4)_3$ molecule and rotation axes used for electrostatic considerations. Small white balls are for hydrogen, light gray (yellow) ones for boron, and gray (fuchsia) is for aluminum. (b) Electrostatic potential energy surface for BH_4 orientation around tri-valent metal cation. Bidentate orientation is for $\alpha=125°06'$ and $\alpha=305°06'$. The energy is given in arbitrary units and normalized to the unity.

C. Electronic properties

The structural and geometrical properties presented above originate from the electronic structure analyzed below. Each compound in the most stable stoichiometry and at the ground state is an insulator with the band gap [highest occupied molecular orbital–lowest unoccupied molecular orbital (HOMO–LUMO gap)] ranging from $E_g=6.53(6.80)$ eV for $Al(BH_4)_3$ through $E_g=4.21(3.99)$ eV for $Sc(BH_4)_3$; $E_g=4.68(4.64)$ eV for $Y(BH_4)_3$; $E_g=(4.13)$ eV for $Ti(BH_4)_4$, and $E_g=5.66(5.72)$ eV for $Zr(BH_4)_4$. $Ti(BH_4)_3$ has a localized state at the Fermi level, due to the remaining electron on *d* shell of titanium. The empty conduction bands are located 1.2 eV above localized state. The electronic density of states (DOS) is presented in Fig. 3. The top of the valence band consists mostly of the occupied states of hydrogen and boron, while the bottom of the conduction band belongs to the empty orbitals of the central metal cation, as presented in Fig. 3. For $Y(BH_4)_3$ the yttrium *p*-states are located just below HOMO. For all compounds, however, an overlap of the electronic states of the metal cation with boron and hydrogen orbitals below the Fermi level can be seen in Fig. 3. Such an overlap indicates that a purely ionic image of these compounds is oversimplified, especially for the transition metals and yttrium. The tridentate BH_4 orientation of these molecules is only weakly perturbed by the electrostatic repulsion of hydrogen.

The band gap and DOS change only weakly for solid state $Al(BH_4)_3$ and $Zr(BH_4)_4$, and only a slight broadening of states due to the formation of periodic structure can be observed. On the other hand for $Sc(BH_4)_3$ and $Y(BH_4)_3$ a significant change in the electronic properties can be observed, especially for the valence band. The solid form of these compounds no longer consists of the molecular units and the formation of the band structure is related to the ionic nature of periodic crystal. The band gap is comparable to HOMO-LUMO gap for molecules.

D. Thermodynamic properties

Equipped with knowledge about the structural and electronic ground-state properties, we examine now the finite-temperature thermodynamics of decomposition/transformation reactions for metal tetrahydroborates. In the simplest case, each compound, in its most stable stoichiometry, may decompose either into elements (or relevant binary metal hydrides) or it may produce a variety of boranes, such as B_2H_6 or higher boranes. As higher boranes, i.e., B_4H_{10}, B_5H_9, $[B_{12}H_{12}]^{2-}$ etc., are thermodynamically more stable than the simplest one—diborane (B_2H_6), we consider as the

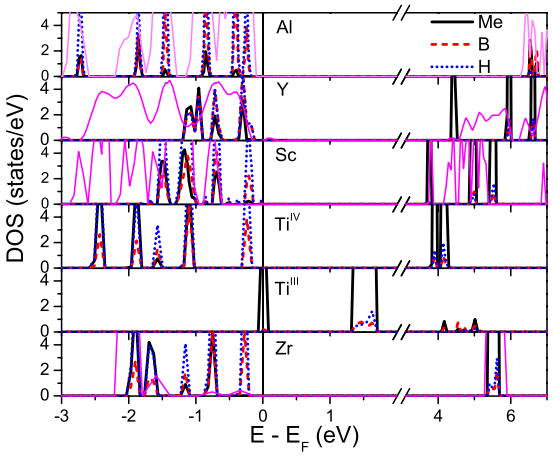

FIG. 3. (Color online) Partial density of states (DOS) for the borohydrides of Al, Sc, Y, Ti, and Zr at $T=0$ K. Solid black lines are for DOS projected on metal cation, dashed red are for projection on boron, dotted for hydrogen. All states are broaden by 0.01 eV. For $Al(BH_4)_3$, $Sc(BH_4)_3$, $Y(BH_4)_3$, and $Zr(BH_4)_4$ total density of states for the solid phase is shown with gray (fuchsia), not in scale, for clarity. Data are presented for the most stable stoichiometry, with exception of titanium where DOS for $Ti(BH_4)_3$ and $Ti(BH_4)_4$ is presented.

TABLE III. Vibrational frequencies (in cm^{-1}) for the most stable stoichiometries of borohydrides of Al, Sc, Y, Ti, and Zr. H_t denotes terminal hydrogen, H_b—the bridge hydrogen between boron and central cation. The second row of each type of hydrogen refers to the solid phase. Two numbers for each mode bracket the range of frequencies. For titanium stoichiometry stable at room temperature is considered.

	$Al(BH_4)_3$	$Sc(BH_4)_3$	$Y(BH_4)_3$	$Ti(BH_4)_3$	$Zr(BH_4)_4$
B-H_t	2535–2627	2624–2626	2611–2613	2637–2639	2626–2630
	2526–2622[a]	2615–2621[b]	2308–2410[c]		2625–2628
	2490–2555[d]	2318–2432[c]	2200–2460[e]	2400–2585[f]	2400–2600[g]
B-H_b	2095–2185	2182–2306	2185–2282	2102–2313	2219–2257
	2098–2196[a]	2205–2399[b]			2220–2261
	2030–2059[d]			2030–2230[f]	2100–2300[g]
M-H_b	1368–1499	1177–1243	1175–1242	1279–1303	1160–1261
	1366–1499[a]	1049–1349[b]	1078–1328[c]		1160–1265
	1425–1565[d]	1047–1320[c]	1145–1340[f]	1210–1345[f]	

[a]For solid $Pn2_1$ structure.
[b]For solid $C222_1$ structure.
[c]For solid $Pa3$ structure.
[d]Reference 11.
[e]Reference 16; for the solid phase.
[f]Reference 57.
[g]Reference 61.

upper stability limit decomposition into metal hydrides, hydrogen, and diborane. In fact, the thermolysis of B_2H_6 leads, via loss of hydrogen, to the formation of boranes that contain more boron and fewer hydrogen atoms in the molecule.[68] In fact, it has been shown recently that very stable solid phases containing $[B_{12}H_{12}]^{2-}$ are formed as intermediates during the decomposition of alkali and alkaline earth metal borohydrides.[23–25] These salts were observed for univalent,[23] and divalent[24,25,69] metal cations. As the *coloso*-boranes can be formed via *Aufbau* process (an addition of BH_4^- to smaller borane clusters), the presence of these species follows directly our assumption that the limiting range of stability is given by decomposition to diborane. We will show that the incorporation of diborane in the decomposition path of the metal tetrahydroborides points out that kinetic effects are important for the discussion about decomposition and stability of these compounds. A possible formation of other intermediate phases, such as metal-boron compounds, is not considered here explicitly, since the formation of stable compounds would lower the thermodynamic stability of metal tetrahydroborates. The compounds investigated here are already unstable at ambient conditions. Formation of salts with $[B_{12}H_{12}]^{2-}$ is not considered explicitly here, as these salts, if exist for metals considered here, would form more stable products than diborane.

Thus for aluminum borohydride the following decomposition paths are considered:

$$Al(BH_4)_3 \Rightarrow AlH_3 + 3B + \frac{9}{2}H_2,$$

which is the lower end of the stability limit. The upper end of the stability limit is related to the formation of aluminum, hydrogen, and diborane:

$$Al(BH_4)_3 \Rightarrow Al + \frac{3}{2}H_2 + \frac{3}{2}B_2H_6,$$

(we consider aluminum and hydrogen, since AlH_3 is thermodynamically unstable at ambient conditions). Decomposition into B_4H_{10} falls between these border regimes.

$$4Al(BH_4)_3 \Rightarrow 4Al + 9H_2 + 3B_4H_{10}.$$

For other metals the decomposition products include: elemental boron, hydrogen or diborane plus binary metal hydrides, MH_2 (M=Sc, Y, Ti, and Zr), since these binary metal hydrides are stable even at several hundred Kelvins.

$$M(BH_4)_n \leftrightarrow MH_2 + nB + \frac{4n-2}{2}H_2,$$

$$M(BH_4)_n \leftrightarrow MH_2 + \frac{n}{2}B_2H_6 + \frac{n-2}{2}H_2,$$

or

$$M(BH_4)_n \leftrightarrow MH_2 + \frac{n}{4}B_4H_{10} + A_nH_2,$$

where n=3 or 4 and A_n=5/2 or 4, respectively. For yttrium we limit our analysis to the formation of YH_2.

To determine the finite temperature properties of each decomposition path the normal modes were calculated for each compound in molecular and solid forms and for each decomposition product. This analysis, besides thermodynamic functions, provides spectroscopic data relevant for infrared and Raman measurements. The high-frequency modes are summarized in Table III. For the molecular form of each compound the range of frequencies for the terminal and bridging hydrogen is in reasonable agreement with the previous stud-

TABLE IV. The zero point energy (ZPE) per formula unit for $M(BH_4)_x$. Values are given in kJ/mol. In the last column the values are for metal hydrides, i.e AlH_3, ScH_2, YH_2, TiH_2, ZrH_2, or for the reference state of H_2, B_2H_6, and B_4H_{10}. The numbers in parentheses correspond to the solid phases of metal tetrahydroborides.

System	$(BH_4)_2$	$(BH_4)_3$	$(BH_4)_4$	MH_x/other
Al	198.28	309.21(312.27)		63.21
Sc	201.25	306.77(317.60)		42.31
Y	199.50	302.65(314.83)	386.05	38.21
Ti	201.39	306.98	409.48	47.93
Zr	200.75	305.48	413.19(413.74)	43.95
H_2				25.95
B_2H_6				161.16
B_4H_{10}				283.72

ies. Note that normal modes for terminal hydrogen in compounds with tridentate BH_4 orientation are located in a rather narrow frequency range close to 2600 cm^{-1}. In the solid forms of $Al(BH_4)_3$ and $Zr(BH_4)_4$ these modes and the ones related to bridging hydrogen remain practically unaltered. For yttrium and scandium borohydrides in the cubic crystalline form the highest frequency modes soften significantly and the modes related to bridging hydrogen disappear, see Table III. For the lowest energy orthorhombic phase of $Sc(BH_4)_2$ phase both high-frequency modes at ~2600 cm^{-1} and those related to bridging hydrogen are present, see Table III. As the highest mode frequency difference between the molecular and solid states exceeds 200 cm^{-1}, it could serve as a simple and robust method for detecting stoichiometric molecular units in compounds or, in the case for scandium borohydride, for discrimination between possible crystalline phases.

The zero point energies (ZPE) for each compound and stoichiometry are presented in Table IV. For each metal borohydride the vibrational contribution to the free energy

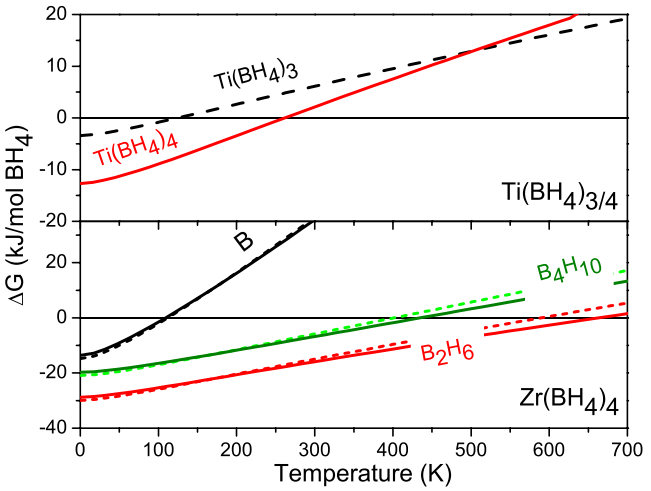

FIG. 5. (Color online) Thermodynamic stability of $Ti(BH_4)_{3/4}$ and $Zr(BH_4)_4$. For titanium borohydride decomposition into TiH_2 and diborane is marked with dashed (black) line for $Ti(BH_4)_3$ and with solid (red) line for $Ti(BH_4)_4$. For zirconium borohydride solid lines denote molecular properties, while the dashed ones are for solid state structures. The decomposition path to boron and hydrogen is marked with black line, to diborane—with red lines and to B_4H_{10}—with green ones. Data is presented for 1 bar partial pressure of hydrogen.

equals ~100 kJ/mol of (BH_4). This rather large value, agrees well with the assumption made by Miwa *et al.* in Ref. 38 for monovalent borohydrides. The formation of solids does not affect ZPE by more than a few %. This is true even for borohydrides of yttrium and scandium, where the molecular structure is destroyed in the ionic crystal.

The free energy for decomposition, i.e., thermodynamic stability of $Al(BH_4)_3$, $Y(BH_4)_3$ and $Sc(BH_4)_3$ is presented in Fig. 4 and for $Ti(BH_4)_3$ and $Zr(BH_4)_4$ in Fig. 5. The negative ΔG is for a temperature range, where metal tetrahydroborates are stable. A particularly striking effect is that all compounds in their molecular states are thermodynamically un-

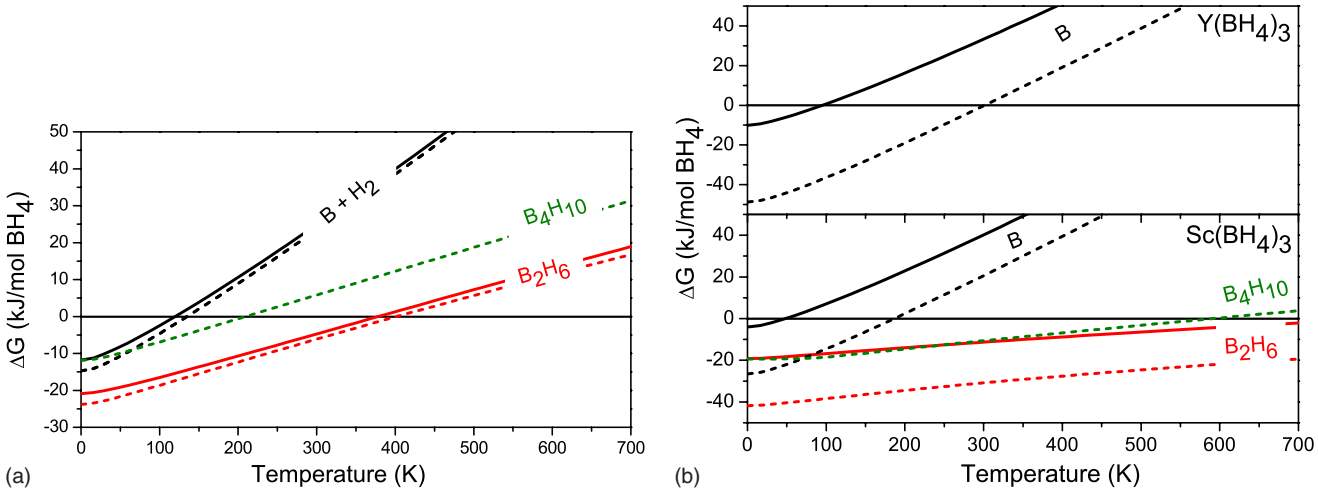

FIG. 4. (Color online) Thermodynamic stability of $Al(BH_4)_3$ (a) and $Y(BH_4)_3$ and $Sc(BH_4)_3$ (b). Solid lines represent data for properties based on a molecular form of compounds, dashed lines represent solid state structures. The decomposition path into boron and hydrogen is marked with a black line, decomposition into diborane—with red lines, and to B_4H_{10} with green ones. Data is presented for 1 bar partial pressure of hydrogen.

stable with respect to decomposition into boron and hydrogen, and they decompose below 150 K at 1 bar partial pressure of hydrogen. Moreover, for borohydrides of aluminum and zirconium there is no difference in thermodynamic stability of their molecular and crystalline forms (due to the weak Van der Waals bonding of these crystals). The stability of crystalline $Y(BH_4)_3$ and $Sc(BH_4)_3$ is significantly larger than the molecular structures due to the large cohesive energy of the crystals. However, the calculated instability of borohydrides of Al, Ti, Sc, and Zr contradicts the experimental observation and characterization of these compounds at ambient conditions. To explain this contradiction we turn our attention to the upper stability limit of metal tetrahydroborates: decomposition into diborane (and higher boranes). Here, the apparent thermodynamic stability of metal borohydrides increases due to positive formation enthalpy of B_2H_6 (ranging from $\Delta H=+36$ kJ/mol to $\Delta H=+52.4$ kJ/mol).[19,70,71] On the other hand, diborane is kinetically robust at ambient conditions. One can see in Figs. 4 and 5 that within decomposition path involving B_2H_6 the compounds with Al, Sc, and Zr become stable at 1 bar of hydrogen and room temperature. The thermodynamic stability range with respect to B_4H_{10} as a final product is located within the border limits bracketed by boron/hydrogen and those of diborane/hydrogen. Even though the detailed decomposition mechanism of metal tetrahydroborates still awaits atomistic explanation, the present results indicate that the stability is related to kinetic factors, as observed for many borohydrides.[72]

Yttrium borohydride in the ionic crystalline structure, is thermodynamically stable with respect to decomposition to YH_2, boron and hydrogen below 300 K (Fig. 4), which is in reasonable agreement with experiential evidence.[16]

The stability of titanium borohydride deserves special consideration as this compound appears to be thermodynamically unstable with respect to decomposition into boron and hydrogen even at the ground state. The stability of $Ti(BH_4)_{3,4}$ with respect to diborane and TiH_2 is presented in Fig. 5. This compound seems to be unstable at normal thermodynamic conditions also for this decomposition path. For the gas phase $Ti(BH_4)_4$ would convert to $Ti(BH_4)_3$ at $T=140$ K, according to harmonic approximation presented here. These results indicate that the difficulties with the synthesis of this compound might be related to the lack of thermodynamic stability of titanium borohydride.

IV. DISCUSSION

In the present paper, we discuss the structural, electronic and thermodynamic properties of metal borohydrides with tri- and tetravalent metal cations. While borohydrides of uni- and divalent metals form strongly ionic solids, the crystalline structure of metal borohydrides with higher valency consists of molecular stoichiometric units of $Al(BH_4)_3$ or $Zr(BH_4)_4$ that are bonded by weak Van der Waals forces. In the weakly bonded crystals each molecular unit is formed via ionic (for $Al(BH_4)_3$), or iono-covalent (for $Zr(BH_4)_4$) forces. However, trivalent cations may also form ionic solids, as for $Y(BH_4)_3$. Crystalline borohydrides of Al, Sc, Y, Ti, and Zr are insulators in their ground state, and as molecules these compounds have the HOMO—LUMO gap exceeding 4 eV. In both molecular and crystalline forms there is a significant charge transfer between metal cation and the surrounding BH_4 groups. The charge transfer ranges between 0.76 e/BH_4 for $Al(BH_4)_3$ and 0.46 e/BH_4 for $Ti(BH_4)_4$. Since the Pauling electronegativity of Ti and Al is comparable (1.54 and 1.61, respectively), the large differences in the charge transfer originate from a different type of bonding between the metal atom and BH_4. A larger orbital overlap for Ti and BH_4 (see, Fig. 3) suggests a more covalent bonding for this compound, and the ionic nature of $Al(BH_4)_3$ is manifested through a bidentate orientation of BH_4 groups in the molecule. This orientation is explained here through a simple electrostatic repulsion of negatively charged hydrogen atoms and presented in Fig. 2. Two aspects of this studies require further discussion: atomic structure and thermodynamic stability of metal borohydrides.

The purpose of the present paper is not to find or propose the most stable crystalline structures for compounds. The present studies are instructive in comparing hypothetical crystalline phases for $Sc(BH_4)_3$, even though scandium borohydride is not interesting for practical large-scale applications, due to high prices and the scarcity of scandium. In a cubic $P3$ symmetry of $Sc(BH_4)_3$ each scandium ion is coordinated to six BH_4 groups with Sc-B distances ranging between 2.58 Å and 2.64 Å. This distance is significantly larger than for a molecular form of this compound, see Table I. On the other hand, in the orthorhombic structure[65] Sc is coordinated to four BH_4 groups with spacing to boron ranging between 2.25 Å, and 2.54 Å, which is close to the respective spacing in the molecular form. The ionic charges in orthorhombic $C222_1$ structure are similar to those in the molecular form, while in the cubic structure these charges are larger, and so are more ionic, see Table II. This suggests that the local interaction between scandium and BH_4 determines the larger stability of the orthorhombic phase.

$Sc(BH_4)_3$ and other metal borohydrides can be considered as ionic systems and the metal coordination in crystalline structures can be explained via a set of Pauling rules.[53,73] Pauling rules state that each cation is surrounded by anions forming regular polyhedron around it. The type of polyhedron depends on the ratio between ionic radii of a cation and an anion. When this ratio is between 0.155 and 0.225, trigonal coordination is preferred; for the ratio between 0.225 and 0.414 tetrahedral coordination is expected; and for the ratio between 0.414 and 0.732 the octahedral coordination is preferred. A sensible ionic radius for BH_4^- is in the range $r_{BH_4}=1.7\ldots2.0$ Å, while those for metals are: $Al^{3+}=0.53(0.675)$ Å; $Sc^{3+}=0.885(1.01)$ Å; $Y^{3+}=1.04(1.16)$ Å; $Ti^{4+}=0.56$ Å, $Ti^{3+}=0.81$ Å, and $Zr^{4+}=0.73(0.86)$ Å,[74] where numbers in the parentheses denote the larger coordination number, i.e., tetrahedral versus trigonal for Al. Within these assumptions a favored coordination for Al and Ti is three to four, and Sc, Y, and Zr possess octahedral coordination in the crystalline ionic form. These simple predictions agree very well with the crystalline coordination of Al, Y, and Zr. The lowest energy structure of scandium borohydride has tetrahedral coordination of Sc, which indicates that nonionic contributions are important for the stability of this

phase or that the real ground state remains to be discovered. The low density of the $C222_1$ phase of $Sc(BH_4)_3$ results from a loose packing of tetrahedra, consisting of Sc and four BH_4 groups, rather than from a denser crystalline packing of borane groups around scandium for $P3$ symmetry.

An important result of the present studies is the indication that at ambient conditions tetrahydroborates of Al, Sc, Ti, and Zr are thermodynamically unstable, with respect to decomposition into molecular hydrogen and boron. To explain the experimental observation of $Al(BH_4)_3$, $Ti(BH_4)_3$, and $Zr(BH_4)_4$ at room temperature we suggest that the stability of these compounds can be explained through a decomposition path that involves the formation of diborane or higher boranes, which have to be formed prior to decomposition into elements. Diborane (B_2H_6) is thermodynamically unstable, i.e., it has positive formation enthalpy ranging from $\Delta H = +36$ kJ/mol to $\Delta H = +52.4$ kJ/mol,[19,70,71] but is kinetically robust even above room temperature.[19,71] If B_2H_6 molecules were formed in an intermediate step of borohydrides decomposition, this would increase their apparent thermodynamic stability. Furthermore, the stability of metal borohydrides considered here would be related to the kinetic factors (those relevant for the stability of diborane). In fact, above 323 K diborane decomposes spontaneously into hydrogen and boranes containing even more boron in the molecules. The decomposition of diborane into monoborane (BH_3) takes place above 573 K, and this molecule decomposes spontaneously into elements above 673 K.[19] The decomposition of borohydrides of mono and divalent metals occurs usually above 500 K. For that reason large amounts of diborane are not observed there. However, careful studies of decomposition products of $LiBH_4$ reveal the presence of B_2H_6.[20] B_2H_6 was also reported as a decomposition product of $Zn(BH_4)_2$ (Ref. 21) or $Zr(BH_4)_4$.[22] Some authors suggest that borohydrides of Zn and Zr decompose slowly at room temperature even though their ultimate decomposition takes place above 300 K.[21,22] This is in accordance with the kinetic stability of borohydrides suggested here.

Based on thermodynamic stability analysis presented above, we suggest that the decomposition of borohydrides of metals with valency higher than two proceeds through the formation of B_2H_6 and H_2. The entropy of such a decomposition path is lower than that for a direct formation of molecular hydrogen and boron, as can be seen in the lower slopes of the free-energy lines in Figs. 4 and 5. The decomposition path can be schematically described as: $M(BH_4)_x \rightarrow MH_2 + \frac{x}{2}B_2H_6 + \frac{x-2}{2}H_2 \rightarrow \cdots \rightarrow MH_2 + xB + \frac{4x-2}{2}H_2$. At high temperatures, where diborane splits into monoborane and further to the elements, the competing decomposition path would involve monoborane: $M(BH_4)_x \rightarrow MH_2 + xBH_3 + \frac{x-2}{2}H_2 \rightarrow \cdots \rightarrow MH_2 + xB + \frac{4x-2}{2}H_2$; "$\cdots$" stands for higher boranes that are formed during the decomposition. The formation enthalpy per BH_4 is presented for $Al(BH_4)_3$ for three decomposition products: boron and H_2, diborane and H_2, and tetraborane plus H_2 in Fig. 6. The formation enthalpy calculated with respect to diborane as a final product of the decomposition path increases the apparent stability of aluminum borohydride. At temperature $T = 200$ K, $Al(BH_4)_3$ is thermodynamically unstable (the positive enthalpy of formation denotes here thermodynamic instability) with respect to the elements and AlH_3. However, it is still stable with respect to emission of diborane, but this is due to the kinetic robustness of B_2H_6.

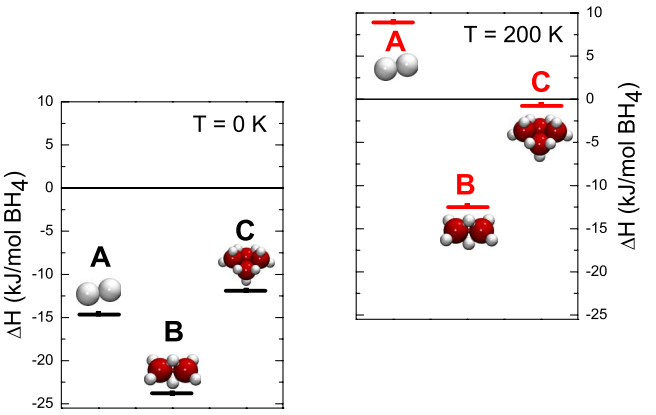

FIG. 6. (Color online) The formation enthalpy of aluminum borohydrides with respect to various decomposition products. A stands for decomposition into boron and hydrogen ($B+H_2$) as a final products; B represents decomposition into diborane and hydrogen ($B_2H_6+H_2$) as final products; and C means decomposition into $B_4H_{10}+H_2$ as an example of higher borane. The left panel shows the enthalpy of decomposition at $T=0$ K, the right panel—$T=200$ K. A schematic view of decomposition products is represented by white balls for hydrogen and dark (red) balls for boron. Data are presented for 1 bar partial pressure of hydrogen.

Higher boranes are spontaneously formed from diborane (usually in the presence of nonoxidizing acids[19]). Thus the decomposition scheme proposed here is in accordance with recent experimental observations of salts with $[B_{12}H_{12}]^{2-}$.[23,24,69] The $[B_{12}H_{12}]^{2-}$ is unusually stable *coloso* borane[72] and is formed during decomposition of uni- and di-valent metal borohyrides at temperatures above 500 K. If these salts existed also for trivalent borohydrides, they would possess stoichiometry $M_2(B_{12}H_{12})_3$ and complex crystalline structures might be expected. However, the question whether $B_{12}H_{12}$ can be formed at lower temperatures or only above 500 K, as in the case of uni- or divalent metals is yet to be answered. The decomposition scheme of $Al(BH_4)_3$ via formation of diborane does not exclude the possible of formation of other aluminoboranes;[75] however, detailed analysis of their stability is beyond the scope of the present paper. Participation of diborane in decomposition of metal tetrahydroborates indicates that kinetic factors are important for considerations about the stability of these compounds, especially at temperatures below 323 K, where B_2H_6 is stable.

V. CONCLUSION

In this manuscript, we show that tetrahydroborides of Al, Sc, Ti, and Zr are thermodynamically unstable at ambient conditions with respect to the decomposition into boron and hydrogen. We suggest that their decomposition path involves as a necessary step the formation of diborane. Thermodynamically unstable B_2H_6 forms higher boranes, possibly including $[B_{12}H_{12}]^{2-}$. The stability of borohydrides of Al, Sc, Ti, and Zr is related to the kinetic factors. Structural and

spectroscopic properties of these compounds are presented and the details of their electronic structure are analyzed. The bonding in the crystalline phases can range from weak Van der Waals for aluminum and zirconium borohydride to ionic for yttrium borohydride.

ACKNOWLEDGMENTS

CPU time allocation at CSCS Supercomputer Center, Manno, Switzerland, and partial support by MNiSW under Project No. N N202 207138 are kindly acknowledged.

*zbigniew.lodziana@ifj.edu.pl

[1] L. Schlapbach and A. Züttel, Nature (London) **414**, 353 (2001).
[2] W. Grochala and P. Edwards, Chem. Rev. **104**, 1283 (2004).
[3] J.-P. Soulié, G. Renaudin, R. Černý, and K. Yvon, J. Alloys Compd. **346**, 200 (2002).
[4] F. Buchter, Z. Łodziana, P. Mauron, A. Remhof, O. Friedrichs, A. Borgschulte, A. Züttel, D. Sheptyakov, T. Strassle, and A. J. Ramirez-Cuesta, Phys. Rev. B **78**, 094302 (2008).
[5] G. Renaudin, S. Gomes, H. Hagemann, L. Keller, and K. Yvon, J. Alloys Compd. **375**, 98 (2004).
[6] R. Černý, Y. Filinchuk, H. Hagemann, and K. Yvon, Angew. Chem., Int. Ed. **46**, 5765 (2007).
[7] J. Her, P. Stephens, Y. Gao, G. Soloveichik, J. Rijssenbeek, M. Andrus, and J. Zhao, Acta Crystallogr., Sect. B: Struct. Sci. **63**, 561 (2007).
[8] F. Buchter *et al.*, J. Phys. Chem. B **112**, 8042 (2008).
[9] E. J. Badin, P. C. Hunter, and R. N. Pease, J. Am. Chem. Soc. **71**, 2950 (1949).
[10] C. Bock, C. Roberts, K. O'Malley, M. Trachtman, and G. J. Mains, J. Phys. Chem. **96**, 4859 (1992).
[11] A. Al-Kahtani, D. L. Williams, J. W. Nibler, and S. W. Sharpe, J. Phys. Chem. A **102**, 537 (1998).
[12] I. Demachy and F. Volatron, Inorg. Chem. **33**, 3965 (1994).
[13] K. Miwa, N. Ohba, S. Towata, Y. Nakamori, A. Züttel, and S. Orimo, J. Alloys Compd. **446**, 310 (2007).
[14] R. M. Rulon and L. S. Mason, J. Am. Chem. Soc. **73**, 5491 (1951).
[15] H. I. Schlesinger, R. T. Sanderson, and A. B. Burg, J. Am. Chem. Soc. **62**, 3421 (1940).
[16] T. Sato, K. Miwa, Y. Nakamori, K. Ohoyama, H.-W. Li, T. Noritake, M. Aoki, S. I. Towata, and S. I. Orimo, Phys. Rev. B **77**, 104114 (2008).
[17] T. Marks and J. Kolb, Chem. Rev. **77**, 263 (1977).
[18] H. Hoekstra and J. Katz, J. Am. Chem. Soc. **71**, 2488 (1949).
[19] N. Wiberg, A. F. Holleman, and E. Wiberg, *Inorganic Chemistry*, 1st ed. (Academic Press, San Diego, USA, 2002).
[20] J. Kostka, W. Lohstroh, M. Fichtner, and H. Hahn, J. Phys. Chem. C **111**, 14026 (2007).
[21] E. Jeon and Y. Cho, J. Alloys Compd. **422**, 273 (2006).
[22] F. Gennari, L. F. Albanesi, and I. Rios, Inorg. Chim. Acta **362**, 3731 (2009).
[23] J.-H. Her, M. Yousufuddin, W. Zhou, S. S. Jalisatgi, J. G. Kulleck, J. A. Zan, S.-J. Hwang, R. C. Bowman, Jr., and T. J. Udovic, Inorg. Chem. **47**, 9757 (2008).
[24] S.-J. Hwang, R. C. Bowman, Jr., J. W. Reiter, J. Rijssenbeek, G. L. Soloveichik, J.-C. Zhao, H. Kabbour, and C. C. Ahn, J. Phys. Chem. C **112**, 3164 (2008).
[25] V. Ozolins, E. H. Majzoub, and C. Wolverton, J. Am. Chem. Soc. **131**, 230 (2009).
[26] G. Kresse and J. Furthmüller, Comput. Mater. Sci. **6**, 15 (1996).
[27] G. Kresse and J. Furthmüller, Phys. Rev. B **54**, 11169 (1996).
[28] P. E. Blöchl, Phys. Rev. B **50**, 17953 (1994).
[29] G. Kresse and D. Joubert, Phys. Rev. B **59**, 1758 (1999).
[30] J. P. Perdew, K. Burke, and M. Ernzerhof, Phys. Rev. Lett. **77**, 3865 (1996).
[31] Z. Łodziana and K. Parlinski, Phys. Rev. B **67**, 174106 (2003).
[32] C. Kittel and H. Kroemer, *Thermal Physics*, 2nd ed. (W.H. Freeman and Company, New York, 1980).
[33] J. E. Northrup, R. Di Felice, and J. Neugebauer, Phys. Rev. B **56**, R4325 (1997).
[34] G. Henkelman, A. Arnaldsson, and H. Jónsson, Comput. Mater. Sci. **36**, 354 (2006).
[35] E. Sanville, S. D. Kenny, R. Smith, and G. Henkelman, J. Comput. Chem. **28**, 899 (2007).
[36] Z. Łodziana and T. Vegge, Phys. Rev. Lett. **93**, 145501 (2004).
[37] T. J. Frankcombe, G. J. Kroes, and A. Züttel, Chem. Phys. Lett. **405**, 73 (2005).
[38] K. Miwa, N. Ohba, S. I. Towata, Y. Nakamori, and S. I. Orimo, Phys. Rev. B **69**, 245120 (2004).
[39] P. Vajeeston, P. Ravindran, A. Kjekshus, and H. Fjellvåg, J. Alloys Compd. **387**, 97 (2005).
[40] R. S. Kumar and A. L. Cornelius, Appl. Phys. Lett. **87**, 261916 (2005).
[41] M. J. van Setten, G. A. de Wijs, and G. Brocks, Phys. Rev. B **77**, 165115 (2008).
[42] V. Ozolins, E. H. Majzoub, and C. Wolverton, Phys. Rev. Lett. **100**, 135501 (2008).
[43] J. Voss, J. S. Hummelshøj, Z. Łodziana, and T. Vegge, J. Phys.: Condens. Matter **21**, 012203 (2009).
[44] Y. Filinchuk, R. Cerný, and H. Hagemann, Chem. Mater. **21**, 925 (2009).
[45] B. Dai, D. S. Sholl, and J. K. Johnson, J. Phys. Chem. C **112**, 4391 (2008).
[46] M. J. van Setten, G. A. de Wijs, M. Fichtner, and G. Brocks, Chem. Mater. **20**, 4952 (2008).
[47] P. Vajeeston, P. Ravindran, and H. Fjellvåg, J. Alloys Compd. **446-447**, 44 (2007).
[48] K. Miwa, M. Aoki, T. Noritake, N. Ohba, Y. Nakamori, S. Towata, A. Züttel, and S. Orimo, Phys. Rev. B **74**, 155122 (2006).
[49] F. Buchter *et al.*, J. Phys. Chem. C **113**, 17223 (2009).
[50] Y. Filinchuk, E. Roennebro, and D. Chandra, Acta Mater. **57**, 732 (2009).
[51] E. H. Majzoub and E. Roennebro, J. Phys. Chem. C **113**, 3352 (2009).
[52] G. Barkhordarian, T. R. Jensen, S. Doppiu, U. Bösenberg, A. Borgschulte, R. Gremaud, Y. Cerenius, M. Dornheim, T. Klassen, and R. Bormann, J. Phys. Chem. C **112**, 2743 (2008).
[53] Z. Łodziana and M. J. van Setten, Phys. Rev. B **81**, 024117 (2010).

[54] Y. Filinchuk, D. Chernyshov, and R. Cerny, J. Phys. Chem. C **112**, 10579 (2008).
[55] Z. Łodziana and T. Vegge, Phys. Rev. Lett. **97**, 119602 (2006).
[56] J. H. Morris and W. E. Smith, J. Chem. Soc., Chem. Commun. **1970**, 245 .
[57] C. Dain, A. Downs, M. Goode, D. Evans, K. Nichols, D. Rankin, and H. Robertson, J. Chem. Soc. Dalton Trans. **1991**, 967.
[58] J. A. Jensen, S. R. Wilson, and G. S. Girolami, J. Am. Chem. Soc. **110**, 4977 (1988).
[59] A. Jarid, A. Lledos, Y. Jean, and F. Volatron, Inorg. Chem. **32**, 4695 (1993).
[60] P. H. Bird and M. R. Churchill, Chem. Commun. (London) **1967**, 403.
[61] L. Forester and W. H. Weinberg, J. Vac. Sci. Technol. **18**, 600 (1981).
[62] A. Haaland, D. J. Shorokhov, A. V. Tutukin, H. V. Volden, O. Swang, G. S. Mcgrady, N. Kaltsoyannis, A. J. Downs, C. Y. Tang, and J. F. C. Turner, Inorg. Chem. **41**, 6646 (2002).
[63] J. C. Green, M. de Simone, M. Coreno, A. Jones, H. M. I. Pritchard, and G. S. McGrady, Inorg. Chem. **44**, 7781 (2005).
[64] S. Aldridge, A. J. Blake, A. J. Downs, R. O. Gould, S. Parsons, and C. R. Pulham, J. Chem. Soc. Dalton Trans. **1997**, 1007.
[65] C. Kim, S.-J. Hwang, R. C. Bowman, Jr., J. W. Reiter, J. A. Zan, J. G. Kulleck, H. Kabbour, E. H. Majzoub, and V. Ozolins, J. Phys. Chem. C **113**, 9956 (2009).
[66] Y. Nakamori, K. Miwa, A. Ninomiya, H. W. Li, N. Ohba, S. I. Towata, A. Züttel, and S. I. Orimo, Phys. Rev. B **74**, 045126 (2006).
[67] J. Plesek and S. Hermanek, Collect. Czech. Chem. Commun. **31**, 3845 (1966).
[68] A. Stock and C. Massenez, Ber. Der Deutschen Chem. Gesellschaft **45**, 3539 (1912).
[69] H.-W. Li, K. Miwa, N. Ohba, T. Fujita, T. Sato, Y. Yan, S. Towata, M. Chen, and S. Orimo, Nanotechnology **20**, 204013 (2009).
[70] L. Gurvich, I. V. Veyts, and C. B. Alcock, *Thermodynamic Properties of Individual Substances*, 4th ed. (Hemisphere, New York, 1989).
[71] C. Housecroft and A. G. Sharpe, *Inorganic Chemistry*, 1st ed. (Pearson Education Limited, Essex, England, 2008).
[72] E. L. Muetterties, J. H. Balthis, Y. T. Chia, W. H. Knoth, and H. C. Miller, Inorg. Chem. **3**, 444 (1964).
[73] L. Pauling, J. Am. Chem. Soc. **51**, 1010 (1929).
[74] R. D. Shannon, Acta Crystallogr., Sect. A: Cryst. Phys., Diffr., Thoer. Gen. Crystallogr. **32**, 751 (1976).
[75] J.-C. Zhao, D. A. Knight, G. M. Brown, C. Kim, S.-J. Hwang, J. W. Reiter, R. C. Bowman, Jr., J. A. Zan, and J. G. Kulleck, J. Phys. Chem. C **113**, 2 (2009).